

# Fluid pressure gradients, arising from oscillations in intramedullary pressure, is correlated with the formation of bone and inhibition of intracortical porosity

Yi-Xian Qin\*, Tamara Kaplan, Anita Saldanha, Clinton Rubin

*Department of Biomedical Engineering, State University of New York at Stony Brook, Stony Brook, NY 11794-2580, USA*

Accepted 27 March 2003

## Abstract

Fluid flow that arises from the functional loading of bone tissue has been proposed to be a critical regulator of skeletal mass and morphology. To test this hypothesis, the bone adaptive response to a physiological fluid stimulus, driven by low magnitude, high frequency oscillations of intramedullary pressure (ImP), were examined, in which fluid pressures were achieved without deforming the bone tissue. The ulnae of adult turkeys were functionally isolated via transverse epiphyseal osteotomies, and the adaptive response to four weeks of disuse ( $n=5$ ) was compared to disuse plus 10 min per day of a physiological sinusoidal fluid pressure signal (60 mmHg, 20 Hz). Disuse alone resulted in significant bone loss ( $5.7 \pm 1.9\%$ ,  $p \leq 0.05$ ), achieved by thinning the cortex via endosteal resorption and an increase in intracortical porosity. By also subjecting bone to oscillatory fluid flow, a significant increase in bone mass at the mid-diaphysis ( $18.3 \pm 7.6\%$ ,  $p < 0.05$ ), was achieved by both periosteal and endosteal new bone formation. The spatial distribution of the transcortical fluid pressure gradients ( $\nabla P_r$ ), a parameter closely related to fluid velocity and fluid shear stress, was quantified in 12 equal sectors across a section at the mid-diaphyses. A strong correlation was found between the  $\nabla P_r$  and total new bone formation ( $r = 0.75$ ,  $p = 0.01$ ); and an inverse correlation ( $r = -0.75$ ,  $p = 0.01$ ) observed between  $\nabla P_r$  and the area of increased intracortical porosity, indicating that fluid flow signals were necessary to maintain bone mass and/or inhibit bone loss against the challenge of disuse. By generating this fluid flow in the absence of matrix strain, these data suggest that anabolic fluid movement plays a regulatory role in the modeling and remodeling process. While ImP increases uniformly in the marrow cavity, the distinct parameters of fluid flow vary substantially due to the geometry and ultrastructure of bone, which ultimately defines the spatial non-uniformity of the adaptive process.

© 2003 Elsevier Ltd. All rights reserved.

**Keywords:** Bone fluid flow; Intramedullary pressure; Remodeling; Strain frequency; Osteoporosis; Strain; Stress; Adaptation; Fluid shear stress; Permeability

## 1. Introduction

Bone's ability to rapidly accommodate changes in its functional environment ensures that sufficient skeletal mass is appropriately placed to withstand the rigors of functional activity, an attribute described as Wolff's Law (Wolff, 1986). The premise of a mechanical influence on bone morphology, now a basic tenet of bone physiology (Lanyon and Baggott, 1976; Carter, 1982; Cowin, 1984; Martin and Burr, 1989; Frost, 1990; Goldstein et al., 1991), indicates that the removal of functional loading is permissive to the loss of bone

(Donaldson et al., 1970; Rubin and Lanyon, 1987), while increased activity (e.g., exercise) will result in increased bone mass (Nilsson and Westlin, 1971; Jones et al., 1977; Krolner et al., 1983; Judex and Zernicke, 2000). Considering the strong anabolic potential of mechanical stimuli, and the devastating consequences of removing it, how the bone cell population perceives and responds to subtle changes in their functional environment remains a key issue in understanding the biological and biomechanical processes of bone remodeling. Further, identifying the regulatory components within the mechanical milieu may prove instrumental in devising a biomechanically based intervention for treating osteoporosis, accelerating fracture healing or promoting bony ingrowth.

\*Corresponding author. Tel.: 631-632-1481; fax: 631-632-8577.

E-mail address: yi-xian.qin@sunysb.edu (Yi-Xian Qin).

In addressing bone's adaptive response to mechanical stimuli, there are a number of different parameters used as the driving function for the optimization process, i.e., strain/stress magnitude, cycle number, number of events, strain tensor and strain energy density. The theories related to strain/stress based bone adaptation range from surface modeling as a function of strain magnitude (Fyhrie and Carter, 1986; Huijkes et al., 1987; Frost, 1990), to time-dependent modeling and remodeling (Beaupre et al., 1990). While there is an overall relationship between intensity of a stimulus and the magnitude of the response, there is very little evidence that the magnitudes of strains or stresses directly correlate to bone's morphological response (Brown et al., 1990; Gross et al., 1997).

It is also important to consider that bone is a highly structured composite material comprised of a collagen-hydroxyapatite matrix and a hierarchical network of lacunae-canalliculi channels. These tunnels permit interstitial flow of fluid through tiny microporosities (Piekariski and Munro, 1977; Weinbaum et al., 1994; Cowin et al., 1995; Cowin, 1999), and thus "by-products" of load, such as the change in fluid velocities or pressures, represent a means by which a physical signal could be translated to the cell (Pollack et al., 1977, 1984; Kelly et al., 1985; Montgomery et al., 1988; Reich et al., 1990; Rubin et al., 1997; Jacobs et al., 1998; Burger and Klein-Nulend, 1999).

To address the potential of this mechanism, load-induced bone fluid flow has been studied both theoretically and experimentally (Pollack et al., 1977, 1984; Gross and Williams, 1982; Montgomery et al., 1988; Reich et al., 1990; Dillaman et al., 1991; Zeng et al., 1994; Weinbaum et al., 1994; Hillsley and Frangos, 1994; Frangos et al., 1996; Jacobs et al., 1998; Tate et al., 1998; Weinbaum, 1998; Burger and Klein-Nulend, 1999; Weinbaum et al., 2001; Mak and Zhang, 2001). Despite the inevitably complex characteristics of fluid flow in porous media (e.g., time and pressure gradient dependent fluid movements), there is early experimental evidence that bone fluid flow driven by loading contributes to the adaptive response, particularly when it is coupled with strain magnitude as well as nutrition supply (Doty and Schofield, 1972; Kelly and Bronk, 1990; Kelly, 1996; Tate et al., 1998). While these experiments demonstrate that cyclic loading can generate significant bone fluid flow as evidenced by streaming potential measurements, there is little evidence to support fluid flow, as opposed to matrix strain, as the driving determinant in bone remodeling, especially under in vivo conditions. This scarcity of data may be associated with the inherent difficulty in separating bone fluid flow induced by mechanical loading from bone matrix strain, as fluid flow certainly is inevitably influenced by bone deformation. However, considering the anabolic potential of low magnitude, high frequency

strain (Rubin et al., 2002), and the strong dependence of fluid flow on loading frequency (Qin et al., 1998; Weinbaum, 1998), it becomes essential to determine if these low-level signals derive some of their regulatory potential through fluid flow rather than matrix deformation.

In previous work, we have shown that intracortical fluid flow is induced not only by bone matrix deformation, but also by the intramedullary pressure (ImP) generated during loading (Qin et al., 2002). Further, we have shown that applying anabolic oscillatory ImP alone can induce transcortical fluid flow as measured by streaming potentials (Qin et al., 2000). The principal goal of this study was to test the hypothesis that bone fluid flow, in the absence of matrix strain, can serve as an anabolic stimulus to bone tissue. This goal was achieved by applying low level, high frequency fluctuations in intramedullary pressure in an avian model of disuse osteopenia.

## 2. Methods

### 2.1. Animals and experimental preparation

All surgical and experimental procedures were approved by the University's Lab Animal Use Committee. Under general halothane anesthesia, the left ulnae of ten adult, one year old, skeletally mature male turkeys were functionally isolated via transverse epiphyseal osteotomies (Qin et al., 1998). The metaphyseal ends of the ulna were covered with a pair of stainless steel caps and fully sealed with 6 ml of polymethylmethacrylate. Two Steinmann pins, 4 mm in diameter and 92 mm in length, were placed through the predrilled holes in the bone and cap unit. This preparation, including the internal caps, pins and external clamps, can prevent mechanical forces from being applied during daily activities, effectively serving to isolate the bone from any mechanical strain. A 4-mm diameter hole was drilled through the cortex at the dorsal side, approximately 1.2 cm from the proximal cap. The hole was tapped and a specially designed fluid loading device, with an internal fluid chamber approximately 0.6 cm<sup>3</sup> in volume, was firmly connected to the bone with an O-ring seal (Fig. 1). A diaphragm was included in the center of the chamber dividing the internal marrow fluid from the external oscillatory loading flow. A surgical plastic tube (2-mm inner diameter), which was connected to the device and passed through the skin, served to couple the device fluid chamber and the external fluid oscillatory loading unit. An injection plug (Terumo Medical Co., Elkton, MD) was connected to the external end of the tube to facilitate fluid flow loading. With the diaphragm and the injection plug, the bone marrow and oscillatory flow media were fully isolated

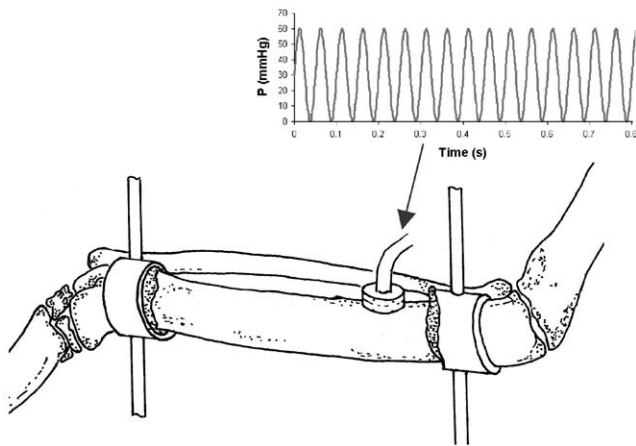


Fig. 1. A diagram of the functionally isolated turkey ulna preparation, such that oscillations in fluid flow can be achieved in the absence of matrix strain. External fixators on the two steel pins at two ends of ulna prevented external mechanical loads. A specially designed device connected into marrow cavity achieved oscillatory fluid loading. A low magnitude and high frequency (60 mmHg, 20 Hz) fluid pressure signal was imposed 10 min daily for 4 weeks in the disuse plus loading group, while the same procedures were prepared for disuse, yet the bone was subject to no exogenous fluid loading.

from the external environment to prevent any infection. To monitor the bone remodeling response, all animals were labeled weekly using tetracycline solution ( $15 \text{ mg} \cdot \text{Kg}^{-1}$ ) through IV. The contralateral ulna served as control.

In addition to the 10 experimental animals, fluid flow was validated via two animals used to calibrate the loading device and its induced pressure magnitude with varied frequencies. The same surgical procedure was used in these animals. An additional tube was connected to the distal end of the ulna. Through this tube, a 50-psi pressure transducer (Entran EPX-10IW) was connected into the medullary canal, thus permitting measurement of the intramedullary pressure during animal rest and applied external ImP loading. The marrow pressures were recorded within the physiological pressure magnitude,  $10 \sim 180 \text{ mmHg}$ , and at a variety of frequencies,  $1 \sim 40 \text{ Hz}$ . The marrow pressure elevated by imposing ImP was then used to calibrate the loading system.

## 2.2. Dynamic fluid flow loading

The animals remained under close supervision until recovery from anesthesia and extensively monitored for an additional 2 h to make certain that they were able to stand normally and resume normal activities. Controlled fluid pressure oscillations started on day two after the surgical preparation. A sinusoidal fluid pressure was applied to the marrow cavity of the ulna at a peak magnitude of  $60 \text{ mmHg}$  at  $20 \text{ Hz}$  for 4 weeks ( $N=5$ ). The remaining animals ( $N=5$ ) were subject to an identical surgical procedure, except that there was no

fluid pressure loading, and thus served to represent disuse.

## 2.3. Quantification of bone remodeling

Following a 10-min period of loading each day for 4 weeks, animals were euthanized via a bolus IV injection of saturated barbiturate. The ulnae of experimental and contralateral control were dissected free of soft tissue, and fixed for 48 h in 70% ethyl alcohol. After dehydration, the pair of ulnae for each animal was carefully positioned in a plastic box and embedded using polymethylmethacrylate.

### 2.3.1. Areal properties

Approximately  $100 \mu\text{m}$  thick sections were cut from the midshaft of the ulnae using a precision diamond wire saw (Well Walter, Model 3241). Each section was microradiographed, scanned at a resolution of 600 dpi with a high-resolution film scanner (Minolta Dimage Scan Multi, Model F-3000, Japan), and converted to a binary image. The final image resolution was approximately  $10 \mu\text{m}/\text{pixel}$ . The cortical area of each fluid loaded ulna was compared to the contralateral control ulna depending on the geometric similarity of the pair of the ulnae (Adams et al., 1995). Endosteal and periosteal new bone formation, as well as intracortical porosity, were traced using custom-written programs (PV-WAVE, Visual Numerics, Boulder, CO). Changes in bone mass, sites of new bone formation and porosity were determined by comparing the adapted area to the bone morphology of the contralateral control ulnae. Since the periosteal surface circumference remained unchanged in disuse bones, morphometric changes were determined by calculating areal differences between contralateral control and disuse alone in each animal. The initial starting point and the orientation of the sectors were based on the orientation of the ventral cortex in the ulna. This orientation is consistent with the turkey ulna anatomy.

In addition to total new bone formation, resorption and porosity changes were approximated using sector analysis in which the bone cross-section was divided into twelve equal angle ( $30^\circ$ ) pie sectors through the centroid of the bone section (Fig. 2) and compared to the animal's contralateral control. The number of sectors was selected by referring to previous studies, e.g., sectors ranged from 6 to 24 (Gross et al., 1997; Judex et al., 1997; Qin et al., 1998). The transcortical fluid pressure gradient was then calculated for each sector as the difference between fluid pressures at the endosteal and periosteal surfaces, where fluid pressure at the periosteal surface was considered zero. More specifically, the pressure gradient was estimated by dividing the averaged linear distance between the periosteal and endosteal surfaces using a total of 30 pairs of points in each

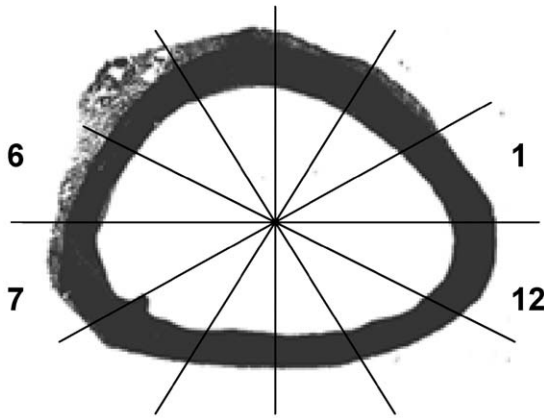


Fig. 2. A mid-diaphyseal cross-section is shown divided into 12 equal-angle sectors. Areal analyses were used to calculate surface bone mass changes and intracortical porosity in each sector. Bone mass changes were evaluated by comparing bone's adaptive responses between an experimental ulna and its contralateral control, as well as within and across experimental groups. An averaged transcortical pressure gradient was calculated in each sector by the pressure difference between endosteal and periosteal surfaces.

sector, where the relation can be expressed by the equation:

$$\nabla P_r = [\text{ImP}]_{\text{peak}} * [\text{cross cortical distance}]^{-1}$$

### 2.3.2. Histomorphometry

Quantification of the cortical modeling/remodeling response to these two distinct stimuli was determined using the distribution of the fluorochrome labels. Histomorphometric evaluation of undecalcified diaphyseal, metaphyseal and epiphyseal sections was performed on a Nikon Labophot system including epifluorescence microscopy, and reflected light microscopy. The fluorescent photomicrographs were taken through the microscope ( $\times 10$ ) and the photographs digitized at 600 dpi using a high resolution SONY digital CCD camera (Model DXC-950P, Japan). The final image resolution was approximately  $1.1 \mu\text{m}/\text{pixel}$ . The image processing was performed using custom-written programs in PV-WAVE. Initial conditions were considered to be the labeling status of the contralateral control bone (Adams et al., 1995). The total area of new labeling and its transcortical distribution were then determined using imaging analysis in PV-WAVE. The magnitude and site specificity of disuse or disuse plus the oscillating fluid flow was determined by quantifying new bone formation at endosteal and periosteal surfaces, as well as porosities within the intracortical region.

### 2.3.3. Statistical analysis

Differences between disuse and disuse plus fluid flow were analyzed using paired student *t*-test. Significance was considered at  $p \leq 0.05$ . Linear regression was used to

identify the relationship between the distributions of fluid parameters and the spatial modeling/remodeling parameters in bone in the fluid flow loading group using *t*-test of the linear regression (Watson, 1992). Thus, the significance of fluid flow on bone was tested in three ways: first, by determining the effective differences between experimental and contralateral control ulnae in both disuse and disuse plus fluid flow groups; second, by testing the significance between disuse and disuse plus fluid flow groups; and third, by correlation between fluid pressure gradient and site-specific response of adaptation in the fluid loading group. A paired two-sample student's *t*-test was performed to determine whether a sample's means were distinct from other criteria.

The contralateral controls in disuse and disuse plus fluid-loading groups served as an intra-animal control. Bone loss caused by disuse was evaluated by comparing experimental and contralateral control ulnae. The fluid-loading group had undergone the same surgical procedure and under the same experimental period as the disuse group. While intra-animal comparison is more accurate and more effective than cross animal comparison, the results of net bone adaptation, morphological loss or gain, were obtained from intra-animal paired data. The final results were explored between groups; between intra-animal experimental and control.

## 3. Results

### 3.1. Changes in areal properties

Morphometric changes in the group subject to disuse alone for 4 weeks indicated a significant loss of bone in the mid-diaphyseal cross sectional area; primarily due to an increase in the percent of the total bone envelope which was porotic ( $5.7 \pm 1.9\%$ , mean  $\pm$  s.d.; total porosity vs. total bone area) as compared to that measured in the contralateral control ( $1.6 \pm 0.7\%$ ;  $p = 0.05$ ) (Fig. 3a,b). There was no evidence of bone resorption at the periosteal surface in any animal. Total area of bone mass (including the area of porosity) in the animals subject to 4-week disuse remained similar between disuse and contralateral control, yielding total cross-sectional areas of  $53.8 \pm 3.5 \text{ mm}^2$  (mean  $\pm$  s.d.) and  $52.7 \pm 2.5 \text{ mm}^2$ , respectively. Morphometric analysis showed that 10-min per day of the oscillating fluid flow resulted in a significant increase in bone mass at the mid-diaphysis ( $18.3 \pm 7.6\%$ ; total new bone/total bone area) ( $p < 0.05$ ), primarily due to periosteal ( $16.1 \pm 6.5\%$ ,  $p < 0.05$ ), as opposed to endosteal ( $2.2 \pm 1.6\%$ ,  $p = 0.13$ ) new bone formation (Fig. 3c).

The sites of modeling and remodeling response in bone were consistent using microradiograph and

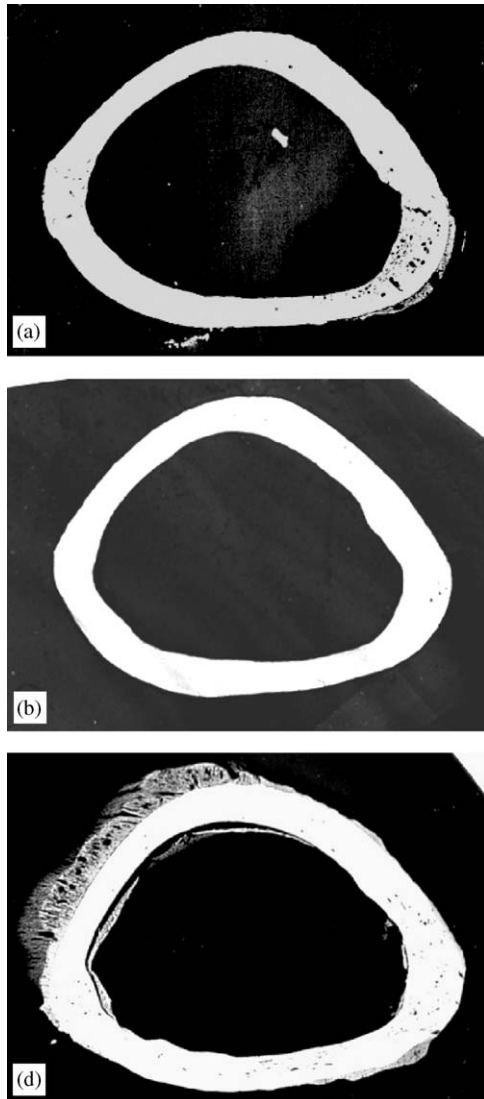


Fig. 3. Microradiographs of (a) animal subject to 4-week disuse resulted in significant bone loss by increase of intracortical porosity. (b) contralateral control of disuse ulna (a). (c) 4-week fluid flow loading resulted in significant new bone formation in periosteal and endosteal surfaces, yielding total of 18% new bone formation as compared to control.

fluorescent labeling analyses, in which new bone formation and intracortical remodeling were identical at the locations of the adaptive response.

### 3.2. Sector specific stimulation of bone adaptation

In animals subject to the fluid pressure oscillations, despite a uniform marrow pressure at the endosteal surface, oscillatory ImP generated non-uniform spatial distributions of transcortical fluid pressure gradients through the cortex, rising 37% from  $4.9 \pm 0.2 \text{ kPa}\cdot\text{mm}^{-1}$  in sectors 1 & 7, to  $6.7 \pm 0.4 \text{ kPa}\cdot\text{mm}^{-1}$  in sectors 5 & 6 (Fig. 4).

Although the ImP stimulus was ultimately non-uniform about the cortex, the non-uniform patterns were consistent between animals. At the periosteal surface, maximum new bone formation was observed in sectors 4, 5 and 6, yielding new bone formation of  $1.7 \pm 0.6 \text{ mm}^2$ ,  $3.1 \pm 1.0 \text{ mm}^2$  (25% & 41% gains, respectively), and  $2.8 \pm 1.2 \text{ mm}^2$  (39% gain) ( $p < 0.02$ ), respectively (Fig. 5). The area of endosteal new bone gain in each sector showed an average gain of  $0.13 \pm 0.08 \text{ mm}^2$  ( $p = 0.13$ ), ranging from a maximum gain of  $0.5 \pm 0.3 \text{ mm}^2$  (7.8% gain in sector) in sector 4, to zero change in sectors 1 & 8. There was no significant difference of endosteal new bone formation among sectors. Oscillatory ImP stimuli resulted in increase of porosity area in each sector from maximum increase of  $0.37 \pm 0.12 \text{ mm}^2$  (6.3%) in sector 12, to a minimum increase of  $0.17 \pm 0.05 \text{ mm}^2$  in sector 5 (Fig. 5).

### 3.3. Correlation between fluid pressure gradient and bone formation

A strong correlation was observed between the transcortical fluid pressure gradient,  $\nabla P_r$ , induced by oscillatory ImP and periosteal new bone formation ( $r = 0.77$ ,  $p = 0.01$ ), as well as total new bone formation ( $12.1 \text{ mm}^2$  gain with 18.3% increase,  $p \leq 0.01$ ) (Figs. 4 and 6). Endosteal new bone formation was weakly correlated with the  $\nabla P_r$  ( $r = 0.53$ ,  $p = 0.08$ ). Interestingly, a negative correlation ( $r = -0.75$ ,  $p = 0.01$ ) was found between increased area of intracortical porosity and  $\nabla P_r$  (Fig. 6).

## 4. Discussion

To determine the regulatory influence of bone fluid flow on the adaptive response of bone, it is necessary to gather both in vitro and in vivo data from a variety of fluid flow conditions. In the past few years, many studies report proliferative responses of osteoblast-like cells, and inhibiting effects on osteoclast-like cells, under pulsing or oscillatory fluid flow loading in culture (Frangos et al., 1996; Rubin et al., 1997; Jacobs et al., 1998; Burger and Klein-Nulend, 1999). For example, oscillatory flow resulted in greater cellular responses than steady flow (Jacobs et al., 1998). These studies unveiled a cellular response to fluid flow loading in an in vitro environment. However, it is possible that the fluid magnitudes examined in these studies were not entirely consistent with those levels which are a fluid representative of physiological levels, e.g., at relatively high pressure magnitudes and at great fluid shear stresses. Further, many studies use immature cells or cells from very young animals, which may not reflect bone cell behavior which could be expected in adults under the conditions of normal mature cell. Finally, it is

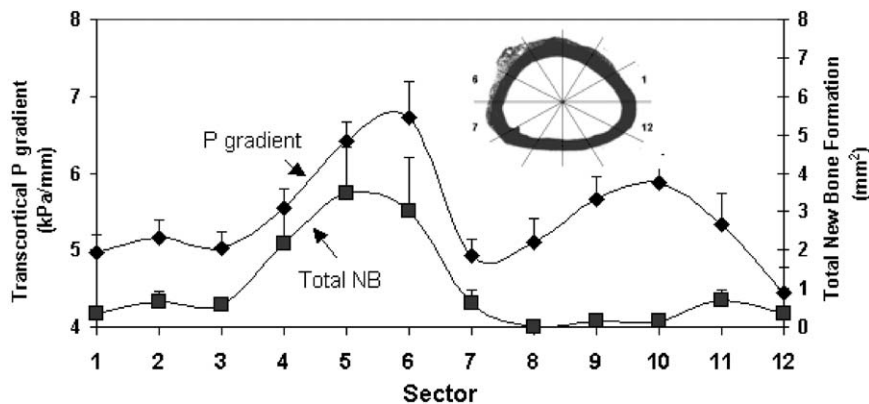


Fig. 4. Mean value ( $\pm$ s.e.) of transcortical fluid pressure gradient distributions for each of 12 sectors in the animals subject to fluid flow loading. Maximum pressure gradient was observed in sector 6, which corresponded to the site of maximal new bone formation. Minimum pressure gradients were located corresponding to least new bone formation sectors, i.e., sector 12 & 7.

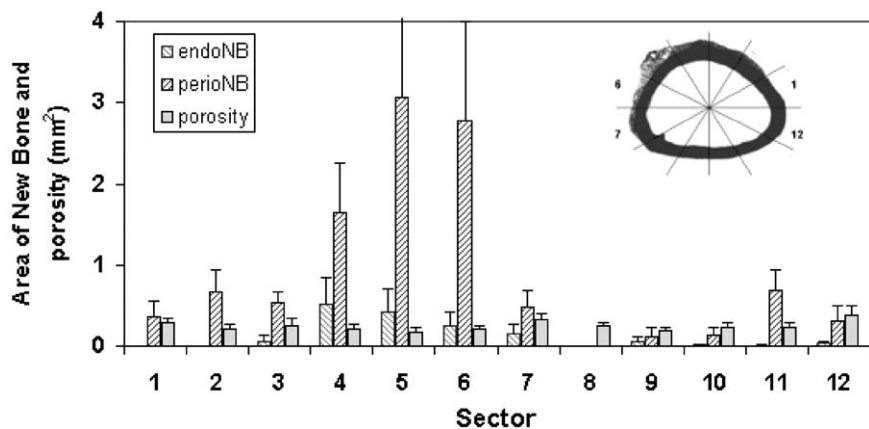


Fig. 5. Spatial distributions, mean ( $\pm$ s.e.), of new bone formation at periosteal and endosteal surfaces as well as an increase in intracortical porosity in each sector. ImP resulted in significantly new bone formation, achieved primarily by periosteal new bone formation ( $p < 0.02$ ). Fluid flow loading also minimized intracortical porosity.

important to consider that in vitro experiments, while proving insight into the mechanism of a cellular response, do not ultimately indicate whether new bone will be formed, or that bone loss can be inhibited. This suggests that knowledge of how bone cells accommodate a systematic, physiologic and morphologically “appropriate” fluid flow environment is important to address the relevance of these signals in controlling bone’s adaptive response. In an attempt to examine the anabolic potential of fluid flow loading in vivo, this study applied oscillatory intramedullary fluid pressure at low magnitude and high frequency, where it was found to stimulate bone formation and reduce bone porosities caused by disuse. This flow stimulus is considered to be physiological in the in vivo flow environment. Thus, if fluid flow is “sufficient,” it is capable of stimulating new bone formation and inhibition of bone resorption with only a daily 10 min period of loading. This implies that physiological fluid flow is indeed a mediator critically involved in bone modeling and remodeling, and that its

influence can be realized in the absence of matrix strain per se.

Given the porous nature of bone, the fluid filled spaces invariably generate a flow upon mechanical loading. In general, load-induced flow and its associated matrix strain are usually coupled. Therefore, segregating the regulatory potential of matrix strain from the anabolic potential of fluid flow becomes inherently difficult. Matrix strain, as a general parameter of bone receiving mechanical loading, is commonly used in describing bone tissue deformation. If bone fluid flow is indeed a key mediator for bone modeling and remodeling, then it is important to test the accommodation of tissues and cells to a customary flow loading environment. This study tried to separate matrix strain and convective fluid flow by dynamically pressurizing the marrow cavity which drives interstitial fluid to flow. The fluid magnitude for such a flow remained in the physiological range generated in the marrow cavity by an animal’s normal activities (Fritton et al., 2000).

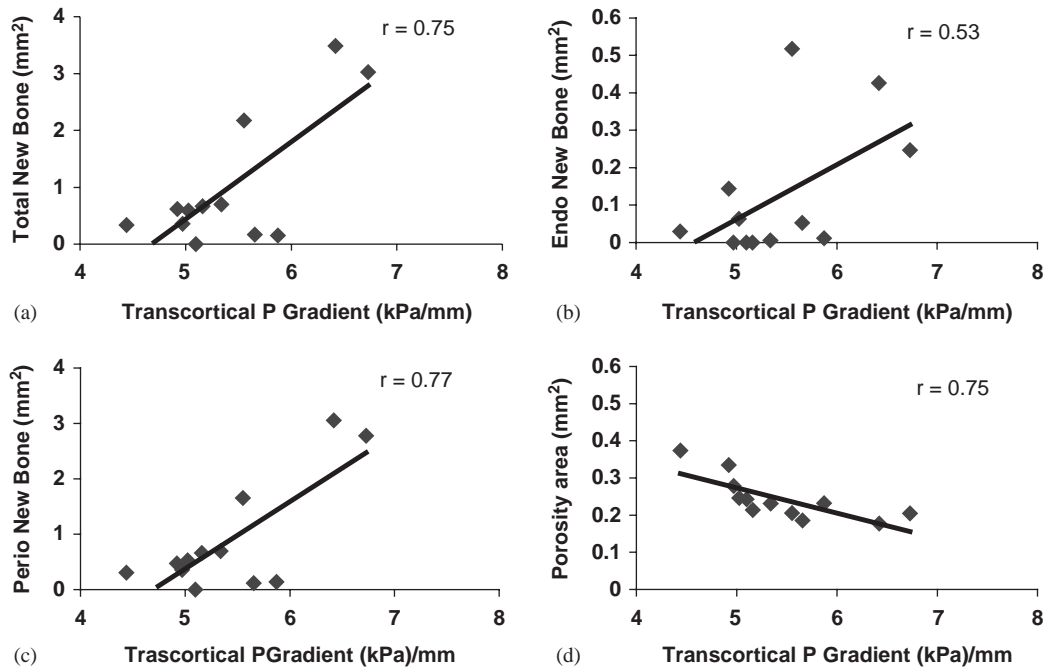


Fig. 6. The strong correlation between calculated pressure gradients and total new bone ( $r = 0.75$ ,  $p < 0.02$ ) (a). While a weak correlation was observed between endosteal new bone formation and pressure gradients ( $r = 0.53$ ) (b), a strong correlation was observed between transcortical fluid pressure gradients and periosteal areal adaptation ( $r = 0.77$ ,  $p < 0.02$ ) (c). A negative correlation was identified between increase in intracortical porosity and increase of transcortical pressure gradients ( $r = 0.75$ ,  $p < 0.02$ ) (d).

When dynamic hydraulic pressure is pressurized in the marrow cavity and interstitial pore space, however, there was concern that the imposed ImP would create deformation in the matrix. Assuming a solid material modulus of 10 GPa and isotropic elastic mechanical behavior of cortical bone, it is estimated that a maximum fluid pressure on the order of 8 kPa will result in approximately  $0.8 \mu\epsilon$  in the matrix. Further, assuming a strain–stress relation in a poroelastic model and a bulk modulus of 5 GPa for the two-phase material, then the calculated matrix strain falls to less than 0.1 microstrain (Neidlinger-Wilke et al., 1994; Cowin, 1999). It is difficult to envision a physical mechanism by which ImP loading resulted in new bone formation could be generated by such small matrix strain, particularly in light of the strong in vitro evidence that fluid flow can perturb to the biological response of bone cells. This experiment suggests that fluid flow can, in and of itself, influence parameters of bone formation and resorption.

The sites of greatest osteogenic response correlated with the greatest gradient of transcortical fluid pressures. The strong correlation between new bone formation and fluid flow suggests that fluid components, i.e., pressure gradients, a close source driving fluid velocity and fluid shear stress, may directly influence the response of bone cells to mechanical stimulation. In addition, the correlation between minimal intracortical porosity and elevated fluid pressure gradients implies

that a basal level of convective bone fluid flow is critical in preserving cortical mass against disuse, such as conditions of bed rest and microgravity. At the very least, it is clear that extremely low-level perturbations of fluid flow, as induced by high frequency oscillations, are providing necessary signals to inhibit intracortical porosity and stimulate new bone formation. Given the anabolic potential of these high frequency signals (Rubin et al., 2002), and the rapid rise in fluid velocities that occur because of high frequencies even in conditions of very low strain (Weinbaum, 1998; Weinbaum et al., 2001), it is certainly possible that signaling the cells responsible for orchestrating bone adaptation is achieved not by subtle changes in matrix strain, but by changes in fluid flow.

The implication of the strong correlation between fluid flow components, i.e., pressure gradients, driven by ImP, is interesting because of its potential to impose fluid shear stress in the cellular environment. A number of theoretical models have been proposed to describe a potential mechanism of fluid pressure and fluid shear stress in bone (Dillaman et al., 1991; Weinbaum et al., 1994; Cowin et al., 1995; Mak et al., 2000), which have been supported by mounting in vitro experimental work (Frangos et al., 1996; Jacobs et al., 1998; Burger and Klein-Nulend, 1999). The effects of an increase in fluid flow induced by oscillatory ImP can potentially influence bone cell activities through several coupling mechanisms. First, raising the ImP can result in a

corresponding increase of outward fluid flow through various fluid pathways, which include the vascular system and the extensive lacunar–canalicular spaces in which the bone cell population resides. Increased fluid velocities can produce fluid shear stresses on the endothelial lining cells of vessels (Girard and Nerem, 1995) and on the bone cells in the lacunar spaces (Weinbaum et al., 1994), where the oscillatory ImP can alter the fluid shear stresses on the cell population and trigger a cellular response. Second, a nutrient pathway for metabolism and the proper disposal of waste products generated from catabolic activities occur through fluid channels. In the soft tissue, molecular diffusion is considered the major pathway for transportation of metabolites (Otter et al., 1999). Because of the relatively dense structure of cortical bone, however, the diffusive mechanism may, in fact, be insufficient to play an adequate role in transporting metabolic constituents between osteocytes and the surrounding vascular canals. An imposed dynamic ImP will enhance this fluid transportation from the blood supply to osteocytes through this convective perfusion mechanism (Piekarski and Munro, 1977; Tate et al., 1998; Wang et al., 2000), where the greatest exchange occurs at sites of greatest pressure gradients.

The fluid magnitude for ImP stimulation was imposed at physiological levels. Via Haversian canals, fluid flow can be modulated by blood flow during ImP stimulation. Blood supply to the long bone is achieved through both marrow and periosteal nutrient vessels, with the main vessel dividing before entering the marrow cavity. The blood supply via the marrow is primarily, but not entirely, centrifugal (Brookes, 1967; Singh and Brookes, 1971; Slater et al., 1991; Churchill et al., 1992; Kiaer, 1994; Bridgeman and Brookes, 1996). The marrow pressure caused solely by the circulation is on the order of 10 to 50 mmHg, depending on the species (Kumar et al., 1979; Bryant, 1983; Otter et al., 1999), and is approximately 18 mmHg in the turkey ulna. While mechanical fading can increase marrow pressure on the order of 150 mmHg with 800~1000 microstrain axial loading, ImP oscillations which can attain pressures of 60 mmHg, would incorporate with the circulatory blood pressure and impact on bone fluid flow. Enhanced fluid convection dependent on either transcortical flows through particular fluid perfusion pathways or altering basal blood flow is supported by the non-uniformity of the surface bone formation.

While physiologic fluid flow showed the potential to initiate the modeling and remodeling process, dynamic components of this fluid may also play an important role in the regulation of adaptation. It is recognized that bone tissues respond very differently to static vs. dynamic load environments, and results in an adapted structure which demonstrates similar peak strain magnitudes during vigorous activity (Lanyon and Rubin,

1984). These regulatory “temporal” components may include strain rate, strain frequency, and strain gradients (O’Connor et al., 1982; Rubin and McLeod, 1994; Turner et al., 1995; Gross et al., 1997; Qin et al., 1998). These temporal components result not only in local matrix deformation, but also in fluid flow, streaming potentials, and other physical phenomena, which also influence cell responses. For example, in the case of the turkey ulna, 10 min of loading per day at 1 Hz requires a peak induced longitudinal normal strain greater than 700  $\mu\epsilon$  to maintain bone mass, while a relatively high frequency (30 Hz) loading regimen reduces this threshold to 70  $\mu\epsilon$  (Qin et al., 1998). The stimulatory effects of fluid flow, driven at physiological magnitude and high frequency but with minimal matrix strain, may depend on the cellular response due to (1) intermittent rather than static flow constant velocity, (2) direct fluid shear stress perturbation, (3) the cumulative effect of small local fluid movements resulting in cells accommodating to large flow cycles, and (4) even an “amplified” effect on the bone cell which could result in pressurization and/or fluid shear stress on the cell (Weinbaum et al., 2001). Again, these data, while not intended to diminish the role of bone strain, imply that anabolic fluid flows, applied in a dynamic manner, can have a tremendous influence on bone mass and morphology even under conditions of extremely low matrix deformations.

That fluid flow results in periosteal expansion in response to intramedullary pressure and transcortical pressure gradients help identify a physical mechanism for the response. Since the periosteum is often referred to as an impermeable layer for fluid perfusion, it is understandable that periosteal modeling requires fluid exchange and/or flow to initiate such an adaptive process. Fluid flow resulted in periosteal bone formation in this study, and thus implies that oscillations of ImP influence bone fluid perfusion and convection in many ways. While the endosteal surface provides an open circulation between marrow pressure and intracortical flow, the interstitial fluid flow in bone must flow out of the mineral to the periosteal surface through a variety of fluid pathways (Morris et al., 1982; Tate et al., 1998; Wang et al., 2000). Since the loading pattern used in these experiments was oscillatory, it may not be necessary that fluid physically flowed out of the periosteal surface but, instead, the oscillation itself may serve as a stimulatory signal. Under oscillatory fluid stimulation, however, a local fluid pressure gradient may be built up with the semi-permeable periosteal boundary condition which will create a flow at the periosteal surface. The spatial distributions of such fluid flow patterns ultimately is dependent on the fluid pressure gradients, defined somewhat by the geometry, ultrastructure and fluid pathways of the bone.

Fluid pressure gradients were calculated based on the assumption of zero pressure magnitude at the periosteal

surface boundary. Using a poroelastic two-phase FEA model, we have previously calculated that transcortical fluid pressure gradients at the periosteal surface were relatively similar when considering either impermeable or semi-permeable surface boundary conditions (Qin et al., 2000). In this particular case, the calculated transcortical pressure gradients may remain proportional regardless of the periosteal permeable conditions, e.g., impermeable vs. semi-permeable. This suggests that the correlation between the morphometric bone formation and the calculated transcortical fluid pressure gradients may be consistent for different permeabilities of the periosteum. However, to better understand interstitial fluid movement, identifying the hydrostatic permeability of cortical bone and the surface boundary conditions are indeed critical. It was found that bone permeability was dependent on many factors, i.e., age and spatial location. Using a canine tibia model, the permeability of puppy tibiae is six times higher than that of adult tibiae (Li et al., 1987). The high permeability of their cortical bone may explain the increase in periosteal new bone formation seen in puppies when a venous tourniquet is applied. While the endosteum is permeable, they have found that the periosteum is, in essence, impermeable unless the periosteal superficial layer is removed in the adult canine tibial cortex. Many tracer studies have indicated that fluid perfusion can penetrate both endosteum and periosteum. Penetration of bone fluid can be greatly enhanced by convection through mechanical loading. It was observed that, in loaded bone, the concentration of tracer dispersed through the mid-diaphysis and surface of the cortex was significantly higher than that which was measured in the unloaded bone (Tate et al., 1998). Nevertheless, to identify the periosteal permeability in this model will help to understand the fluid flow pattern in bone through the convection mechanism. This may be important for future work.

There were several other limitations in the study. Like many in vivo studies, this protocol required an invasive surgical preparation, which potentially altered the bone metabolism and introduced complications during fluid loading. To minimize the variability that inevitably occurs in a biological system, the influence of the surgical procedure might, to a certain degree, be determined by the sham group and the contralateral control. In addition, the fluid loading hole was located on the dorsal side of the ulna. The hole was physically 3 cm away from the midshaft where the cross sectional morphometric analysis was performed. This distance exceeds the threshold of a surgical procedure inducing bone modeling/remodeling activity. In addition, there were distinct limitations in relying on the analytical analysis, in which it is necessary to simplify what is undoubtedly a complex biological system. There are several fluid filled spaces in the cortical structure, e.g.,

Haversian channel, lacuna-canalliculi, and micropore space. The calculation of fluid pressure gradients was based on the assumption of uniform distributions of these porosities in bone. Although accurately determining the true distributions of fluid channels and porosity of cortical bone is immensely difficult, the potential inaccuracy can be modified with further determined spatial distribution of pore size and permeabilities.

In conclusion, in an effort to determine how bone tissue senses fluid flow related stimuli, and their importance to the adaptive response in bone, we have developed an animal model which can induce oscillatory fluid flow in the absence of bone matrix deformation. The results indicate that small perturbations of basal fluid flow can influence both bone formation and resorption. New bone formation on the periosteal surface was strongly correlated to fluid pressure gradients, suggesting the adaptive response to be influenced by both fluid velocity and shear force. These data also suggest that maintaining anabolic cortical fluid flow is essential to maintain intracortical bone mass against the effects of disuse. The results imply that the fluid flow induced by physiological values is essential and important in retaining bone quality and quantity, and that small fluctuations in fluid flow, achieved via pressure differentials, has potential for therapeutic applications against skeletal disorders even in the absence of mechanical strain.

### Acknowledgements

This work is kindly supported by The Whitaker Foundation (RG-99-24, Qin), and The US Army Medical Research and Materiel Command (DAMD-17-02-1-0218, Qin). The author is grateful to Ms. Marilyn Cute for her excellent technical assistance.

### References

- Adams, D.J., Pedersen, D.R., Brand, R.A., Rubin, C.T., Brown, T.D., 1995. Three-dimensional geometric and structural symmetry of the turkey ulna. *Journal of Orthopaedic Research* 13, 690–699.
- Beaupre, G.S., Orr, T.E., Carter, D.R., 1990. An approach for time-dependent bone modeling and remodeling—application: a preliminary remodeling simulation. *Journal of Orthopaedic Research* 8, 662–670.
- Bridgeman, G., Brookes, M., 1996. Blood supply to the human femoral diaphysis in youth and senescence. *Journal of Anatomy* 188 (Pt 3), 611–621.
- Brookes, M., 1967. Blood flow rates in compact and cancellous bone, and bone marrow. *Journal of Anatomy* 101, 533–541.
- Brown, T.D., Pedersen, D.R., Gray, M.L., Brand, R.A., Rubin, C.T., 1990. Toward an identification of mechanical parameters initiating periosteal remodeling: a combined experimental and analytic approach. *Journal of Biomechanics* 23, 893–905.

- Burger, E.H., Klein-Nulend, J., 1999. Mechanotransduction in bone—role of the lacuno-canalicular network. *FASEB Journal* 13 (Suppl.), S101–S112.
- Bryant, J.D., 1983. The effect of impact on the marrow pressure of long bones in vitro. *Journal of Biomechanics* 16, 659–665.
- Carter, D.R., 1982. The relationship between in vivo strains and cortical bone remodeling. *Critical Reviews of Biomedical Engineering* 8, 1–28.
- Churchill, M.A., Brookes, M., Spencer, J.D., 1992. The blood supply of the greater trochanter. *Journal of Bone Joint Surgery [British]* 74, 272–274.
- Cowin, S.C., 1984. Mechanical modeling of the stress adaptation process in bone. *Calcified Tissue Interaction* 36 (Suppl. 1), S98–S103.
- Cowin, S.C., 1999. Bone poroelasticity. *Journal of Biomechanics* 32, 217–238.
- Cowin, S.C., Weinbaum, S., Zeng, Y., 1995. A case for bone canaliculi as the anatomical site of strain generated potentials. *Journal of Biomechanics* 28, 1281–1297.
- Dilaman, R.M., Roer, R.D., Gay, D.M., 1991. Fluid movement in bone: theoretical and empirical. *Journal of Biomechanics* 24 (Suppl.1), 163–177.
- Donaldson, C.L., Hulley, S.B., Vogel, J.M., Hattner, R.S., Bayers, J.H., McMillan, D.E., 1970. Effect of prolonged bed rest on bone mineral. *Metabolism* 19, 1071–1084.
- Doty, S.D., Schofield, B.H., 1972. Metabolic and structural changes with osteocytes of rat bone. *Calcium, Parathyroid Hormone and the Calcitonins*. Excerpta Medica, Amsterdam, pp. 353–364.
- Frangos, J.A., Huang, T.Y., Clark, C.B., 1996. Steady shear and step changes in shear stimulate endothelium via independent mechanisms—superposition of transient and sustained nitric oxide production. *Biochemical and Biophysical Research Communications* 224, 660–665.
- Fritton, S.P., McLeod, K.J., Rubin, C.T., 2000. Quantifying the strain history of bone: spatial uniformity and self-similarity of low-magnitude strains. *Journal of Biomechanics* 33, 317–325.
- Frost, H.M., 1990. Skeletal structural adaptations to mechanical usage (SATMU): 2. Redefining Wolff's law: the remodeling problem. *Anatomical Record* 226, 414–422.
- Fyhrie, D.P., Carter, D.R., 1986. A unifying principle relating stress to trabecular bone morphology. *Journal of Orthopaedic Research* 4, 304–317.
- Girard, P.R., Nerem, R.M., 1995. Shear stress modulates endothelial cell morphology and F-actin organization through the regulation of focal adhesion-associated proteins. *Journal of Cellular Physiology* 163, 179–193.
- Goldstein, S.A., Matthews, L.S., Kuhn, J.L., Hollister, S.J., 1991. Trabecular bone remodeling: an experimental model. *Journal of Biomechanics* 24 (Suppl. 1), 135–150.
- Gross, D., Williams, W.S., 1982. Streaming potential and the electromechanical response of physiologically-moist bone. *Journal of Biomechanics* 15, 277–295.
- Gross, T.S., Edwards, J.L., McLeod, K.J., Rubin, C.T., 1997. Strain gradients correlate with sites of periosteal bone formation. *Journal of Bone Mineral Research* 12, 982–988.
- Hillsley, M.V., Frangos, J.A., 1994. Review: bone tissue engineering: the role of interstitial fluid flow. *Biotechnology and Bioengineering* 43, 573–581.
- Huiskes, R., Weinans, H., Grootenboer, H.J., Dalstra, M., Fudala, B., Slooff, T.J., 1987. Adaptive bone-remodeling theory applied to prosthetic-design analysis. *Journal of Biomechanics* 20, 1135–1150.
- Jacobs, C.R., Yellowley, C.E., Davis, B.R., Zhou, Z., Cimbala, J.M., Donahue, H.J., 1998. Differential effect of steady versus oscillating flow on bone cells. *Journal of Biomechanics* 31, 969–976.
- Jones, H.H., Priest, J.D., Hayes, W.C., Tichenor, C.C., Nagel, D.A., 1977. Humeral hypertrophy in response to exercise. *Journal of Bone Joint Surgery [America]* 59, 204–208.
- Judex, S., Zernicke, R.F., 2000. High-impact exercise and growing bone: relation between high strain rates and enhanced bone formation. *Journal of Applied Physiology* 88, 2183–2191.
- Judex, S., Gross, T.S., Zernicke, R.F., 1997. Strain gradients correlate with sites of exercise-induced bone-forming surfaces in the adult skeleton. *Journal of Bone Mineral Research* 12, 1737–1745.
- Kelly, P.J., 1996. Is osteoporosis a genetically determined disease? *British Journal of Obstetrics and Gynaecology* 103 13(Suppl.), 20–26.
- Kelly, P.J., Bronk, J.T., 1990. Venous pressure and bone formation. *Microvascular Research* 39, 364–375.
- Kelly, P.J., An, K.N., Chao, E.Y.S., Rand, J.A., 1985. Fracture healing: biomechanical, fluid dynamic and electrical considerations. *Bone Mineral Research*. Elsevier, New York, pp. 295–319.
- Kiaer, T., 1994. Bone perfusion and oxygenation. Animal experiments and clinical observations. *Acta Orthopaedica Scandinavica* 257 (Suppl.), 1–41.
- Krolner, B., Toft, B., Pros, N.S., Tondevold, E., 1983. Physical exercise as prophylaxis against involuntional vertebral bone loss: a controlled trial. *Clinical Science (London)* 64, 541–546.
- Kumar, S., Davis, P.R., Pickles, B., 1979. Bone-marrow pressure and bone strength. *Acta Orthopaedica Scandinavica* 50, 507–512.
- Lanyon, L.E., Baggott, D.G., 1976. Mechanical function as an influence on the structure and form of bone. *Journal of Bone Joint Surgery [British]* 58-B, 436–443.
- Lanyon, L.E., Rubin, C.T., 1984. Static vs dynamic loads as an influence on bone remodelling. *Journal of Biomechanics* 17, 897–905.
- Li, G.P., Bronk, J.T., An, K.N., Kelly, P.J., 1987. Permeability of cortical bone of canine tibiae. *Microvascular Research* 34, 302–310.
- Mak, A.F., Zhang, J.D., 2001. Numerical simulation of streaming potentials due to deformation-induced hierarchical flows in cortical bone. *Journal of Biomechanical Engineering* 123, 66–70.
- Mak, A.F., Qin, L., Hung, L.K., Cheng, C.W., Tin, C.F., 2000. A histomorphometric observation of flows in cortical bone under dynamic loading. *Microvascular Research* 59, 290–300.
- Martin, R.B., Burr, D.B., 1989. *Structure Function and Adaptation of Compact Bone*. Raven Press, New York.
- Montgomery, R.J., Sutker, B.D., Bronk, J.T., Smith, S.R., Kelly, P.J., 1988. Interstitial fluid flow in cortical bone. *Microvascular Research* 35, 295–307.
- Morris, M.A., Lopez-Curto, J.A., Hughes, S.P., An, K.N., Basingthwaite, J.B., Kelly, P.J., 1982. Fluid spaces in canine bone and marrow. *Microvascular Research* 23, 188–200.
- Neidlinger-Wilke, C., Wilke, H.J., Claes, L., 1994. Cyclic stretching of human osteoblasts affects proliferation and metabolism: a new experimental method and its application. *Journal of Orthopaedic Research* 12, 70–78.
- Nilsson, B.E., Westlin, N.E., 1971. Bone density in athletes. *Clinical Orthopaedics* 77, 179–182.
- O'Connor, J.A., Lanyon, L.E., MacFie, H., 1982. The influence of strain rate on adaptive bone remodelling. *Journal of Biomechanics* 15, 767–781.
- Otter, M.W., Qin, Y.X., Rubin, C.T., McLeod, K.J., 1999. Does bone perfusion/reperfusion initiate bone remodeling and the stress fracture syndrome? *Medical Hypotheses* 53, 363–368.
- Piekarski, K., Munro, M., 1977. Transport mechanism operating between blood supply and osteocytes in long bones. *Nature* 269, 80–82.
- Pollack, S.R., Korostoff, E., Sternberg, M.E., Koh, J., 1977. Stress-generated potentials in bone: effects of collagen modifications. *Journal of Biomedical Materials Research* 11, 670–677.
- Pollack, S.R., Salzstein, R., Pienkowski, D., 1984. Streaming potential in fluid filled bone. *Ferroelectrics* 60, 297–309.
- Qin, Y.X., Rubin, C.T., McLeod, K.J., 1998. Nonlinear dependence of loading intensity and cycle number in the maintenance of bone

- mass and morphology. *Journal of Orthopaedic Research* 16, 482–489.
- Qin, Y.X., Lin, W., Rubin, C.T., 2002. The pathway of bone fluid flow as defined by in vivo intramedullary pressure and streaming potential measurements. *Annals of Biomedical Engineering* 30, 693–702.
- Qin, Y.X., McLeod, K., Rubin, C.T., 2000. Intracortical fluid flow is induced by dynamic intramedullary pressure independent of matrix deformation. 46, 740. 2000. 46th Annual Meeting of Orthopaedic Research Society.
- Reich, K.M., Gay, C.V., Frangos, J.A., 1990. Fluid shear stress as a mediator of osteoblast cyclic adenosine monophosphate production. *Journal of Cellular Physiology* 143, 100–104.
- Rubin, C.T., Lanyon, L.E., 1987. Kappa Delta Award paper Osteoregulatory nature of mechanical stimuli: function as a determinant for adaptive remodeling in bone. *Journal of Orthopaedic Research* 5, 300–310.
- Rubin, C.T., McLeod, K.J., 1994. Promotion of bony ingrowth by frequency-specific, low-amplitude mechanical strain. *Clinical Orthopaedics* 165–174.
- Rubin, J., Biskobing, D., Fan, X., Rubin, C., McLeod, K., Taylor, W.R., 1997. Pressure regulates osteoclast formation and MCSF expression in marrow culture. *Journal of Cellular Physiology* 170, 81–87.
- Rubin, C., Turner, A.S., Muller, R., Mitra, E., McLeod, K., Lin, W., Qin, Y.X., 2002. Quantity and quality of trabecular bone in the femur are enhanced by a strongly anabolic, noninvasive mechanical intervention. *Journal of Bone and Mineral Research* 17, 349–357.
- Singh, M., Brookes, M., 1971. Bone growth and blood flow after experimental venous ligation. *Journal of Anatomy* 108, 315–322.
- Slater, R.N., Spencer, J.D., Churchill, M.A., Bridgeman, G.P., Brookes, M., 1991. Observations on the intrinsic blood supply to the human patella: disruption correlated with articular surface degeneration. *Journal of the Royal Society of Medicine* 84, 606–607.
- Tate, M.L., Niederer, P., Knothe, U., 1998. In vivo tracer transport through the lacunocanalicular system of rat bone in an environment devoid of mechanical loading. *Bone* 22, 107–117.
- Turner, C.H., Owan, I., Takano, Y., 1995. Mechanotransduction in bone: role of strain rate. *American Journal of Physiology* 269, E438–E442.
- Wang, L., Cowin, S.C., Weinbaum, S., Fritton, S.P., 2000. Modeling tracer transport in an osteon under cyclic loading. *Annals of Biomedical Engineering* 28, 1200–1209.
- Watson, J.V., 1992. *Flow Cytometry Data Analysis, Basic Concepts and Statistics*. Cambridge University Press, New York.
- Weinbaum, S., 1998. 1997 Whitaker Distinguished lecture: models to solve mysteries in biomechanics at the cellular level; a new view of fiber matrix layers. *Annals of Biomedical Engineering* 26, 627–643.
- Weinbaum, S., Cowin, S.C., Zeng, Y., 1994. A model for the excitation of osteocytes by mechanical loading-induced bone fluid shear stresses. *Journal of Biomechanics* 27, 339–360.
- Weinbaum, S., Guo, P., You, L., 2001. A new view of mechanotransduction and strain amplification in cells with microvilli and cell processes. *Biorheology* 38, 119–142.
- Wolff, J., 1986. *The Law of Bone Remodeling*. Springer, Berlin.
- Zeng, Y., Cowin, S.C., Weinbaum, S., 1994. A fiber matrix model for fluid flow and streaming potentials in the canaliculi of an osteon. *Annals of Biomedical Engineering* 22, 280–292.